Predicting Geophysical Measurements: Testing a Combined Empirical and Model-Based Approach using Surface Waves

Michael E. Pasyanos
Geophysics and Global Security Division
Lawrence Livermore National Laboratory
P.O. Box 808, L-205
Livermore, CA 94551-0808
phone: (925) 423-6835, FAX: (925) 423-4077
email: pasyanos@s74.es.llnl.gov

Abbreviated title: Predicting Geophysical Measurements

ABSTRACT

There are several approaches commonly used to provide spatial corrections of geophysical data. One end-member approach is to develop model-based corrections in which the variations are based on either *a priori* knowledge or based on geophysical inversions, such as tomography. While this approach would have the advantage of full spatial coverage, in general one would be unable to recover the full station corrections due to the inherent averaging of models. Another end-member approach, common in seismically active regions, would be to develop empirically based corrections based directly on measurements. An example of this approach would be kriging or other interpolation techniques. The advantage of this approach is a true fit to the most applicable measurements, but at the cost of severe spatial limitations. Ideally, one would like to combine the two approaches. This paper demonstrates the value of a combined empirical and model-based approach to generating accurate spatial correction surfaces using surface wave measurements and a tomography model from the Middle East and North Africa. By kriging residual values from a tomographic model, there was a significant reduction in misfit over either approach alone. In principle, kriging measurement residuals from models could improve many geophysical applications from travel times to amplitudes.

Keywords: kriging, Bayesian, surface waves, group velocity, tomography, interpolation

INTRODUCTION

Geophysical applications often require the determination of the value of a parameter at a particular location. For example, to locate an event one needs to be able to calculate travel times from any given point in the earth to a station. Most simply this is done using a travel time curve based on a one-dimensional model, but to most accurately locate an event, one needs to account for the structural variability of the earth. At a seismic station this might take the form of a "source-specific site-correction" (SSSC) or more simply a "correction surface," which in various forms have long been used to improve event locations (e.g. Herrin and Taggart, 1966). Such a correction surface maps the variability of the parameter out in graphical form as seen at a specific station. One could also make correction surfaces of other parameters, for example seismic amplitudes, for use in making detection maps, improving earthquake-explosion discriminants, or estimating hazard. In this short note, I will use the example of surface wave group velocities. Accurate estimates of the expected group velocity at a station are quite useful for forming phase-matched filters. These filters allow accurate estimates of the maximum surface wave magnitude M_s and have applications in monitoring the Comprehensive Nuclear-Test-Ban Treaty (e.g. Stevens and Adams, 1999, Pasyanos *et al.*, 2000).

There are two end-member approaches commonly used to provide spatial corrections of geophysical data. One approach to develop a correction surface is by directly interpolating measured correction data points. This would be an example of a measurement or empirical-based correction surface. An illustration of this approach would be kriging or other interpolation techniques. Given the nature of earthquake occurrence, seismological problems are often beset with a non-uniform distribution of data. In seismically active regions one tends to have many measurements, whereas in aseismic regions, there are few, if any, measurements. In such cases, it is desirable to have an interpolation algorithm that can work on highly non-uniform and sparse data sets. One successful technique that has been applied to several geophysical data sets is non-stationary Bayesian kriging (Schultz *et al.*, 1998). Kriging methods use a statistical approach to interpolation that provides uncertainties in the interpolation estimate. This technique has now been commonly applied to a number of geophysical data sets including travel-time corrections used in seismic event locations (Myers and Schultz, 1999) and path corrections for regional phase amplitudes (Phillips, 1999, Rodgers *et al.*, 1999). An advantage of the empirically based approach is a true fit to the most applicable measurements, but at the cost of severe spatial limitations.

Where no direct measurements exist, the correction surface reverts to a background model, usually based on a trend underlying the data.

The other end-member approach is to develop corrections in which the variations are based on either an *a priori* model or a model based on geophysical inversions. This is an example of a model-based approach to constructing correction surfaces. Suitable models to use for such a methodology could be either tomographic inversion models or models based on geophysical inference such as 3SMAC (Nataf and Ricard, 1996) and CRUST5.1 (Mooney *et al.*, 1998). A model of this type specifically developed for the Middle East and North Africa is the MENA model (Sweeney and Walter, 1998). While this approach would have the advantage of full spatial coverage, in general one would be unable to recover the full station corrections due to the inherent averaging and unmodeled complexity of inversion techniques and models.

Ideally, one would like to combine both approaches in order to make use of the advantages of each. In ordinary kriging, residuals are formed by taking the observations against the best unbiased mean estimate of the local observed data. In intrinsic kriging, residuals are formed by comparing the observations to a more general estimate of the mean, such as a low-order polynomial. As described in Schultz *et al.* (1998), the real power of intrinsic kriging comes from using a reliable *a priori* background model as an estimate of the local mean.

This study represents a demonstration of the power of this technique for Rayleigh wave group velocity measurements in the Middle East and North Africa. Using this particular data set, a model derived from a large surface wave tomography is employed as a background model from which to interpolate individual station corrections. Results are then compared to both ordinary kriging and to the original model with the goal of measurement predictability. A particular advantage of kriging in the surface wave case is that the residuals relative to the tomographic model may contain the signatures of anisotropy that are averaged out in the tomography. Group velocity travel-time correction surfaces can be used to create suitable phase-matched filters in order to extract weak surface-wave signals from noise. This is particularly useful in treaty monitoring and verification where the surface-wave magnitude M_s can be combined with body-wave magnitude m_b to form one of the best known discriminants of earthquakes and explosions (Stevens and Day, 1985).

It should be stressed, however, that while the demonstration of this methodology presented here is for surface wave group velocities this technique should be applicable to any number of geophysical techniques involving spatial corrections. While the group velocity travel times can be used to improve surface wave signals, this same methodology is

also applicable to travel time corrections of other seismic phases (i.e. P, P_n, S) which can be used to improve seismic event locations. Amplitude corrections could be applied to regional discriminants (e.g. P_n/L_g, P_g/L_g, P_n/S_n) or to mapping predictions of seismic hazard measurements such as peak ground accelerations.

DATA

Surface wave group velocity data is used in this study to present the method and demonstrate its applicability. The correction surface used for both the model-based approach and the background model for the kriging that is employed in the combined empirical/model-based approach is derived from a group velocity tomography of the Middle East and North Africa (Pasyanos *et al.*, 2000). Using broadband data gathered from various sources, they measured group velocity using a multiple narrow-band filter (e.g. Herrmann, 1973). Figure 1 shows the source-receiver paths that were measured for 20 second Rayleigh waves. Calibrating group velocities near 20 seconds is important since surface wave magnitudes are generally measured at or near this period. Overall, there are about 4000 measurements at this period. Path coverage is excellent throughout the Mediterranean Sea, Arabian Peninsula, and Middle East, with many crossing paths. Coverage is poorer in North Africa, East Africa and Northern Eurasia with crossing paths but a lower path density. Finally, the path coverage is worst in West Africa and out into the Atlantic and Indian Oceans where there are fewer crossing paths.

From these measurements, a tomographic inversion of the data set is performed using a conjugate gradient technique (Pasyanos *et al.*, 2000). Results for 20 second Rayleigh waves are presented in Figure 2, showing the significant group velocity variations. Group velocities at this period are sensitive to continental / oceanic crust transitions, as well as the influence of sedimentary basins. For example, extremely fast group velocities are found out in the Atlantic and Indian Oceans as well as along the spreading ridges of the Gulf of Aden and Red Sea. Slow velocities are found in the eastern Mediterranean, Black Sea, Caspian Sea, Persian Gulf and Mesopotamian Foredeep, all locations of deep sedimentary basins. In all, there is a range in group velocities from around -15% to 25% about the mean velocity, or about a 40% variation in total.

Using the tomography results, one can form a velocity correction surface that can then be used as a background model for the kriging. The correction surface has been formed by simultaneously solving multiple path integrals from a station to points along a regular grid. Figure 3 shows the surface for 20 second Rayleigh waves at Geoscope station TAM in

Tamanrasset, Algeria. Here the predicted correction surface varies with azimuth. Towards the south, the 20 second group velocities are fast, due to the fast crust and minimal sediment cover of Africa. This is particularly true in the southwest direction, towards the West African Craton. To the north, the slower velocities of the sedimentary–rich Mediterranean Basin temper the fast group velocities of Africa. Small "wakes" of slow velocity can be seen behind the eastern Mediterranean Sea and the Caspian Sea. It should be emphasized that these wakes are not due to smearing as in the case of an inversion, but rather due to the continuing influence on velocities in back of large anomalies. Fast wakes can be seen in back of the Red Sea and Gulf of Aden. The fastest velocities can be found in areas farthest into oceanic crust. Due to the averaging inherent in generating the correction surface, the velocity variations are less than the tomography, spanning from about –10% to 10% from the mean.

In addition to the correction surface prepared for a station, there are the actual measurements recorded at the station. These are the measurements to use as the basis for the spatial kriging. In all, there are about 300 measurements of 20 second Rayleigh wave group velocity at station TAM. They are illustrated by the colored triangles shown in Figure 3. Large differences between the measurements and the background model are due to the inadequacy of the model-based correction approach caused by the inherent averaging and unmodeled complexity described earlier.

KRIGING

The kriging algorithm is applied to the data by first forming residuals of the measurements that have been made at our target station TAM. This is done in two different ways. In the first case, the residuals are formed by comparing them against the mean group velocity of our data set (in this case 2.93 km/s) in the customary manner of ordinary kriging. These residuals are then used in the kriging algorithm and the mean removed from the measurements is then added back to produce the 20 second group velocity surface. The resulting correction surface is shown in Figure 4. Like the background model that has been derived from the tomography, the correction surface has generally slow group velocities from events in the Middle East, moderate velocities from the Mediterranean, and fast velocities from along the oceanic ridges. In general, the interpolated output is able to accommodate the changes in the group velocity where measurements exist. In regions where the measurements are consistent, there is also low variance. Note, however, that where there aren't any measurements (i.e. most of North Africa, the southern Former Soviet

Union), the correction surface returns to the mean value. This is a problem if the correction surface will be applied to new data, which may exist outside of areas where one has currently made measurements.

In the second case, the residuals are formed by differencing the observations and predictions from the tomography model. These residuals are now used in the kriging and the background model is subsequently added to the results. Figure 5 shows the group velocity correction surface made with this method. Once again the correction surface corresponds very well with the individual measurements in regions where there are direct data measurements. Outside of these regions, however, one can see major differences between the two results. Instead of smoothly returning to the mean model, the correction surface returns to the tomographically derived background model, making this figure look a lot like Figure 3. For example, in regions like West Africa and portions of the oceans away from the ridges, where there are no data points, this correction surface predicts fast group velocities. Using this process, one should be better able to forecast velocities in regions where no data measurements exist because the group velocities are based on a tomography which has sampled these regions, albeit not directly at station TAM. Furthermore, models should not be limited only to tomographic inversions. In fact, in cases of very limited data, *a priori* models of a region could serve as a basis for the background model.

RESULTS

In order to assess the predictability of the three methods presented above, a series of tests were performed to measure the misfit of the models to the data. In the first case, the residuals for each data point are simply calculated against the value predicted from the mean model. For the other cases, however, a different approach was taken in order to avoid measuring the residuals on data that had been used to calculate the correction surface – employing a ten-fold cross-validation technique. More specifically, ten realizations of the data have been made, each time leaving out a different 10% of the data points. The surface wave tomography was performed for each realization of the data, and correction surfaces were made from the tomography. While new tomography models were produced for each new realization to avoid circularity, in practice the models (and model-derived correction surfaces) did not change significantly by removing 10% of the TAM data. The two corrections surfaces generated from the kriging (calculated against the mean model and the background model) were produced for each realization. These correction surfaces were then used to measure the residuals for the portion of the data that had been removed. The

residuals for the next set of data points were calculated in the second realization, and so on, until residuals were calculated for each data point. In this way, special care has been made not to measure the misfit of any datum that was used in developing the surface in order to avoid circularity. The advantage of a cross-validation technique that tests 10% of the data instead of one point at a time in the typical "leave-one-out" approach is that one can more reliably assess the performance of the methods in regions having only a few measurements.

Figure 6 shows the results of the residual analysis. The first histogram plots the travel-time residuals of the mean model. Notice the bimodal distribution of the residuals that represent dominantly continental and oceanic paths. The RMS of the residuals is 0.225 km/s. The second histogram shows the residuals of the kriging performed using the mean velocity model as the background model and is therefore representative of empirically based corrections. The RMS of the data residuals in this case is 0.108 km/s or a 77% variance reduction from the model mean. The third histogram shows the residuals of the background model derived from the tomography and represents model-based corrections. The RMS of the residuals is 0.100 km/s or an 80% variance reduction. Finally, the bottom right histogram shows residuals of the kriging performed using the tomographic model as the background model. In this case, the RMS is 0.08 km/s or an 86% variance reduction from the mean. Viewed from a different perspective, the combined empirical and model-based approach achieves another 40% variance reduction vs. the empirically based corrections alone or another 30% variance reduction vs. the model-based corrections alone. The very significant reduction in the residuals demonstrates the advantage of using the combined model/empirical technique. Similar tests were performed at other stations in the Middle East and North Africa. The hybrid technique yielded variance improvements ranging from 15% - 35% compared to the background model and 25% - 45% against kriging alone.

To summarize, here is the basic approach that was used to develop the correction surfaces. First, an appropriate background model for the parameter is found (or created). The model can either be derived from tomography or by using a suitable *a priori* model. Next, the residuals of the direct measurements made at the station are formed against the background model, removing long-wavelength changes in the local mean. These residuals are then interpolated using kriging or other suitable methods. The background model is then added back to the interpolation results to produce the final correction surface. The same approach can be performed for discrimination (amplitudes) and location (P-waves and S-waves).

CONCLUSIONS

Kriging is a robust and reliable algorithm used to spatially interpolate non-uniform and sparse observations and is, therefore, ideally suited for many seismic problems. A variety of methods can be used to form the residuals used in the kriging. By forming them against a mean background velocity, it is possible to retrieve accurate velocities in the vicinity of our measurements. Such empirically based corrections, however, are often spatially limited and are unable to predict velocities outside of the narrow regions with measurements. Using a background model based on the tomography, one is better able to produce more realistic and reliable correction surfaces away from the measurement points. In regions where direct measurements of the data are available, the empirically based approach would dominate. Where direct measurements are unavailable, one would need to rely more on the model-based approach. This approach represents an effort to strike a balance between the two end-member methodologies.

The predictability of the combined approach, as measured by data variance, significantly exceeds that of empirical and model-based measurements alone. One should also be able to employ tomographic models, or even *a priori* models as the background model for spatial interpolation. As a general methodology, this hybrid approach should be applicable to many geophysical data sets involving spatial corrections. In the future, it would be useful to assess the performance of the combined approach to other types of data, such as phase velocities, travel times, and body and surface wave amplitudes.

Acknowledgments. Bill Walter, Craig Schultz, Artie Rodgers, and Steve Myers provided critical reviews of the manuscript and supplied me with the kriging algorithms used in the study. Helpful suggestions were provided by reviewer Aaron Velasco. Figures were generated using the Generic Mapping Tools (GMT) software (Wessel and Smith, 1998). This work was performed under the auspices of the U.S. Department of Energy at the Lawrence Livermore National Laboratory under contract number W-7405-ENG-48. This is LLNL contribution UCRL-JC-136022.

REFERENCES

Herrin, E., and J. Taggart (1966). Epicenter Determination for the Salmon Event, *J. Geophys. Res.*, **71**, 3503-3506.

Herrmann, R. B. (1973). Some Aspects of Band-pass Filtering of Surface Waves, *Bull. Seism. Soc. Am.*, **63**, 663-671.

Mooney, W.D., G. Laske, and T.G. Masters (1998). CRUST 5.1: A global crustal model at 5° X 5°, *J. Geophys. Res.*, **103**, 727-747.

Myers, S.C., and C.A. Schultz (1999). Improving sparse-network seismic location with Bayesian kriging and teleseismically constrained calibration events, in press, *Bull. Seism. Soc. Am.*

Nataf, H.-C., and Y. Ricard (1996). 3SMAC: an a priori tomographic model of the upper mantle based on geophysical modeling, *Phys. Earth Planet. Inter.*, ***95***, 101-122.

Pasyanos, M.E., W.R. Walter, and S.E. Hazler (2000). A surface wave dispersion study of the Middle East and North Africa for Monitoring the Comprehensive Nuclear-Test-Ban Treaty, in press, *Pure and Appl. Geophys.*

Phillips, W.S. (1999). Empirical path corrections for regional-phase amplitudes, *Bull. Seism. Soc. Am.*, **89**, 384-393.

Rodgers, A.J., W.R. Walter, C.A. Schultz, S.C. Myers, and T. Lay. (1999). A comparison of methodologies for representing path effects on regional P/S discriminants, *Bull. Seism. Soc. Am.*, **89**, 394-408.

Schultz, C., S. Myers, J. Hipp, and C. Young (1998). Nonstationary Bayesian kriging: a predictive technique to generate corrections for detection, location, and discrimination, *Bull. Seism. Soc. Am.*, **88**,1275-1288.

Stevens, J. and D.A. Adams (1999). Improved methods for regionalized surface wave analysis, *21st Seismic Research Symposium on Monitoring a CTBT*, 274-282.

Stevens, J.L., and S.M. Day (1985). The physical basis of m_b:M_s and variable frequency magnitude methods for earthquake/explosion discrimination, *J. Geophys. Res.*, **90**, 3009-3020.

Sweeney, J.J., and W. Walter (1998). Preliminary definition of geophysical regions for the Middle East and North Africa, *UCRL-ID-132899*, Lawrence Livermore National Laboratory, Livermore, California, 41 pp.

Wessel, P., and W.H.F. Smith (1998*)*. New, improved version of Generic Mapping Tools released, *EOS Trans. Amer. Geophys. U*., **79**, 579.

Figure captions

Figure 1. Map of the Middle East / North Africa region showing 20 second Rayleigh wave group velocity path distribution. Circles indicate events, triangles indicate stations, and lines indicate source-receiver paths used in the inversion.

Figure 2. Group velocity tomography made from group velocity measurements shown in Figure 1. The color scheme varies from slow (red) to fast (purple) with areas of poor resolution shown in faded colors.

Figure 3. The correction surface of 20 second Rayleigh waves for station TAM derived from the tomography results. The colored triangles illustrate actually group velocity measurements made at that station.

Figure 4. The correction surface for station TAM made using kriging algorithm with the residuals formed against mean. The colored triangles are the same as in Figure 3.

Figure 5. The correction surface for station TAM made using kriging algorithm with residuals formed against background model derived from tomography results. The colored triangles are the same as in Figures 3 and 4.

Figure 6. Histograms of measurement residuals for mean velocity model, empirically based corrections, model-based corrections, and combined empirical and model-based corrections. In each histogram, the y-axis represents the frequency-percentage of the total number of measurements. RMS is the root-mean-square of the data variance.

20 second Rayleigh

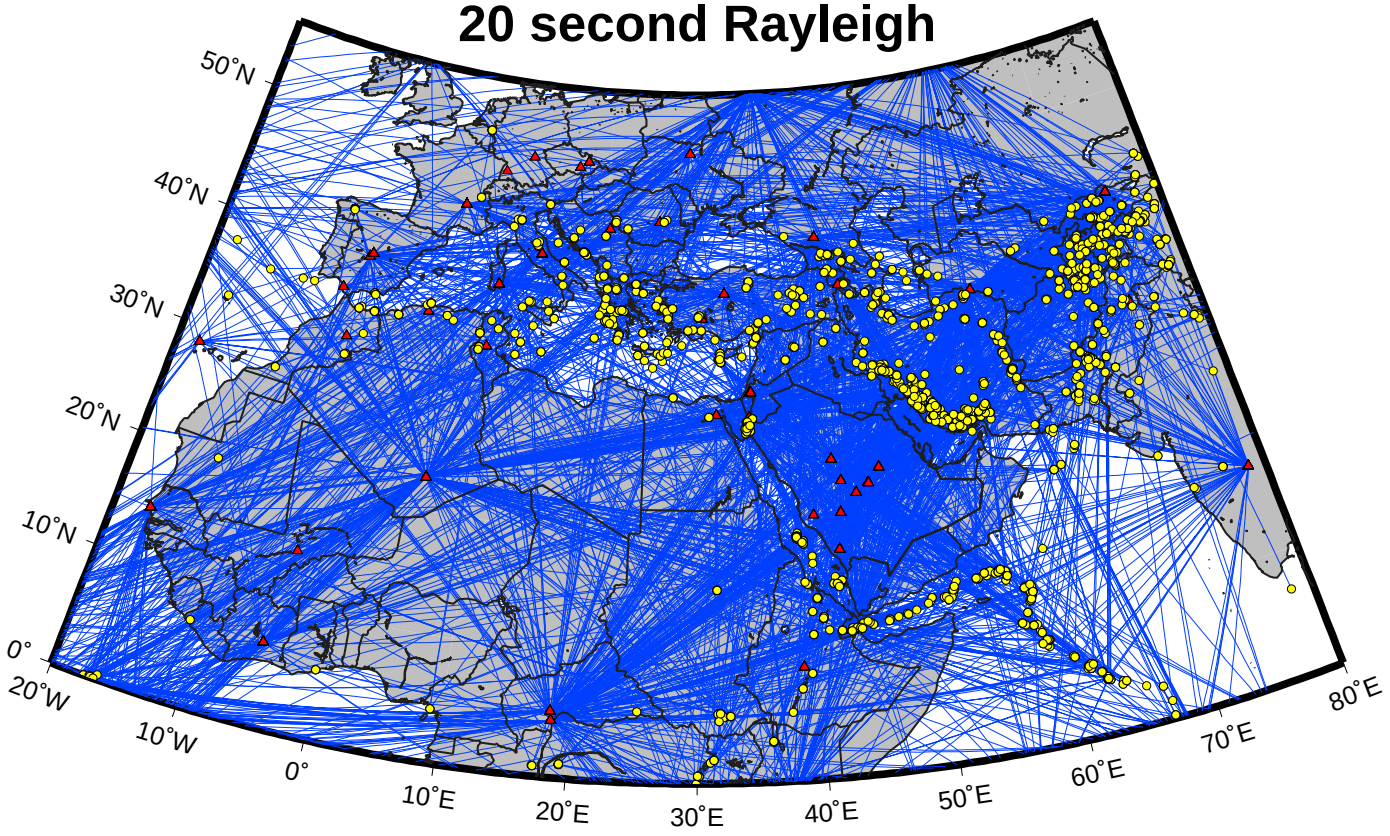

20 second Rayleigh

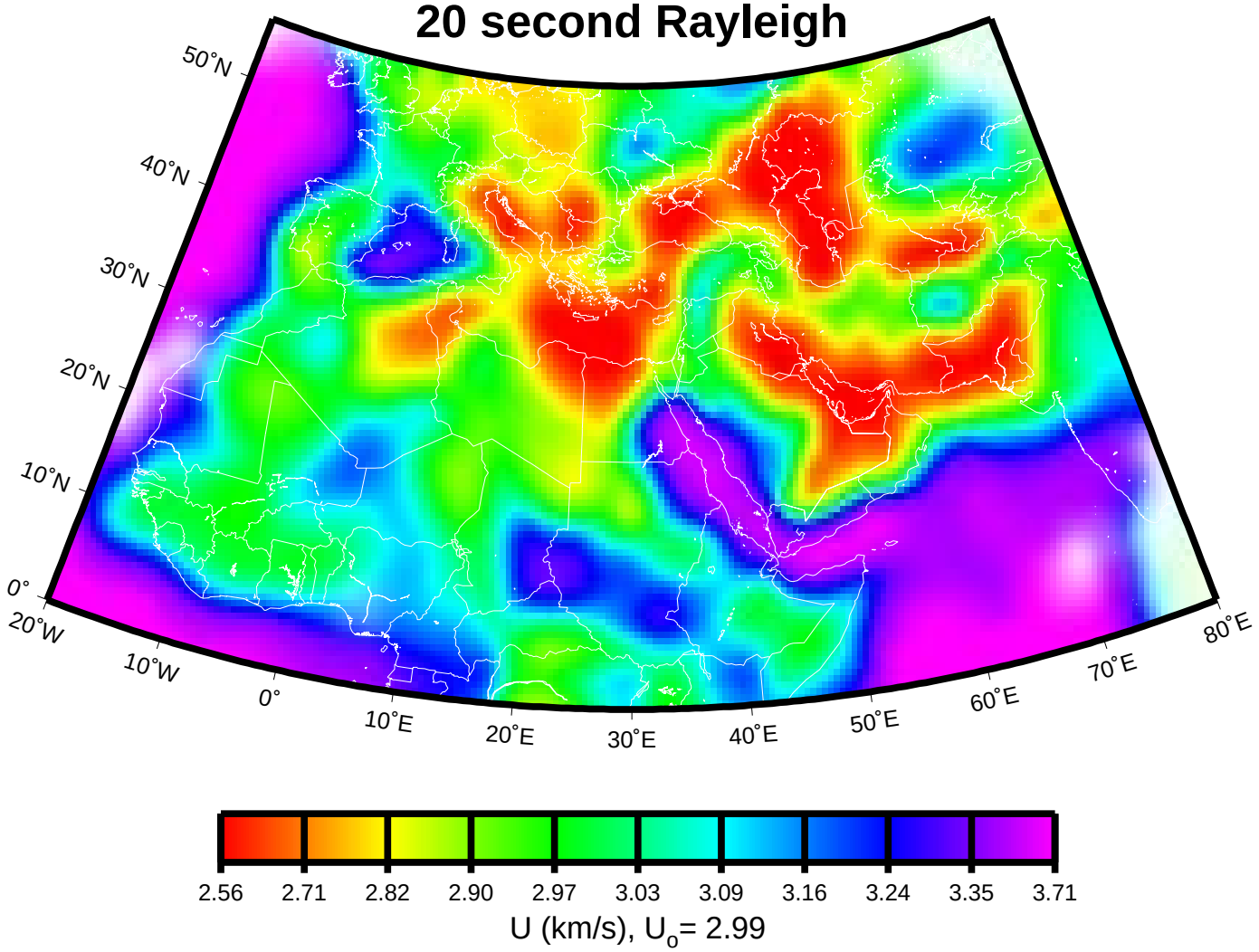

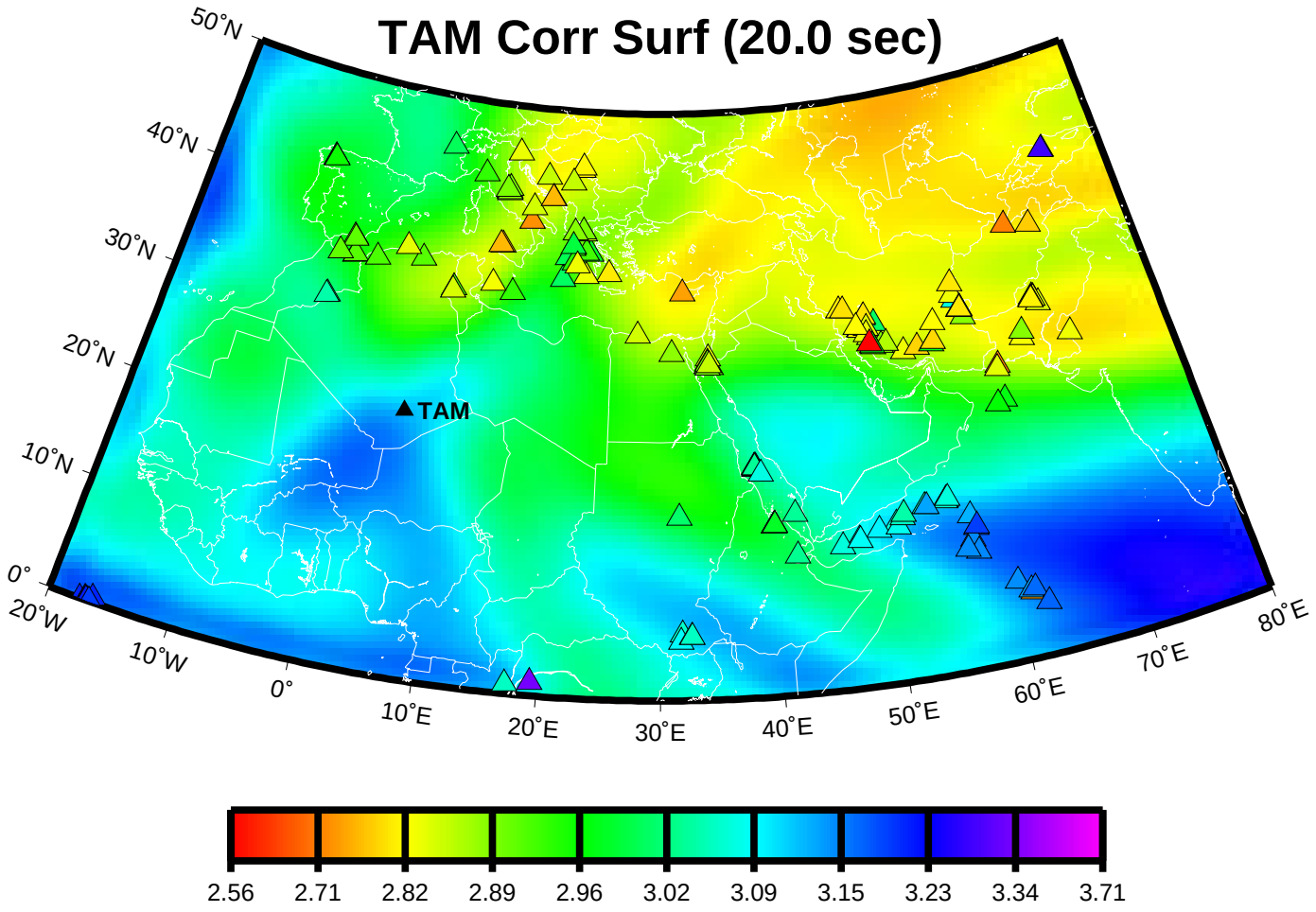
TAM Corr Surf (20.0 sec)
50°N
40°N
30°N
20°N
10°N
0°
20°W
10°W
0°
10°E
20°E
30°E
40°E
50°E
60°E
70°E
80°E
TAM
2.56
2.71
2.82
2.89
2.96
3.02
3.09
3.15
3.23
3.34
3.71

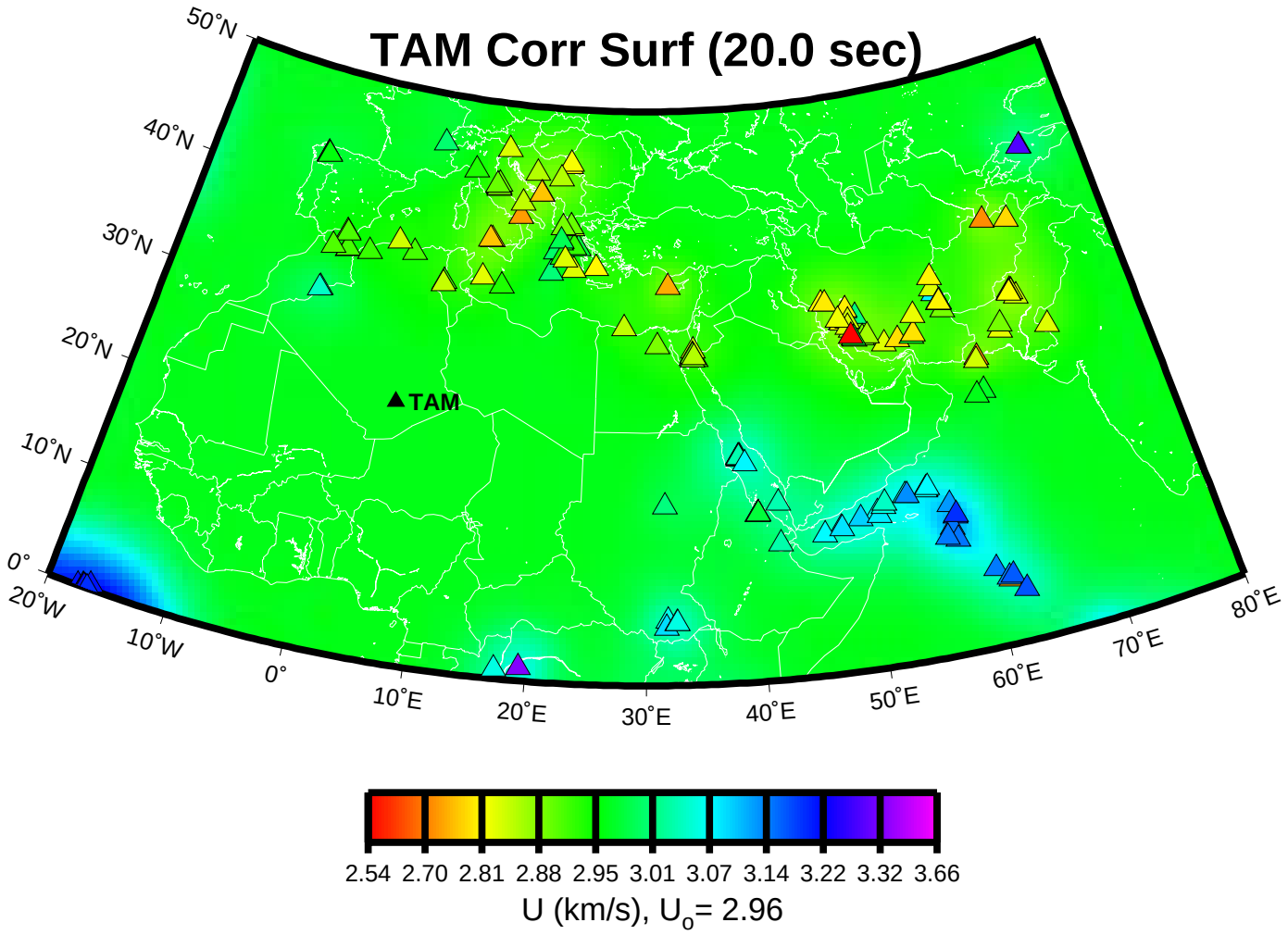
TAM Corr Surf (20.0 sec)
50°N
40°N
30°N
20°N
10°N
0°
20°W
10°W
0°
10°E
20°E
30°E
40°E
50°E
60°E
70°E
80°E
TAM
2.54 2.70 2.81 2.88 2.95 3.01 3.07 3.14 3.22 3.32 3.66
U (km/s), U$_o$= 2.96

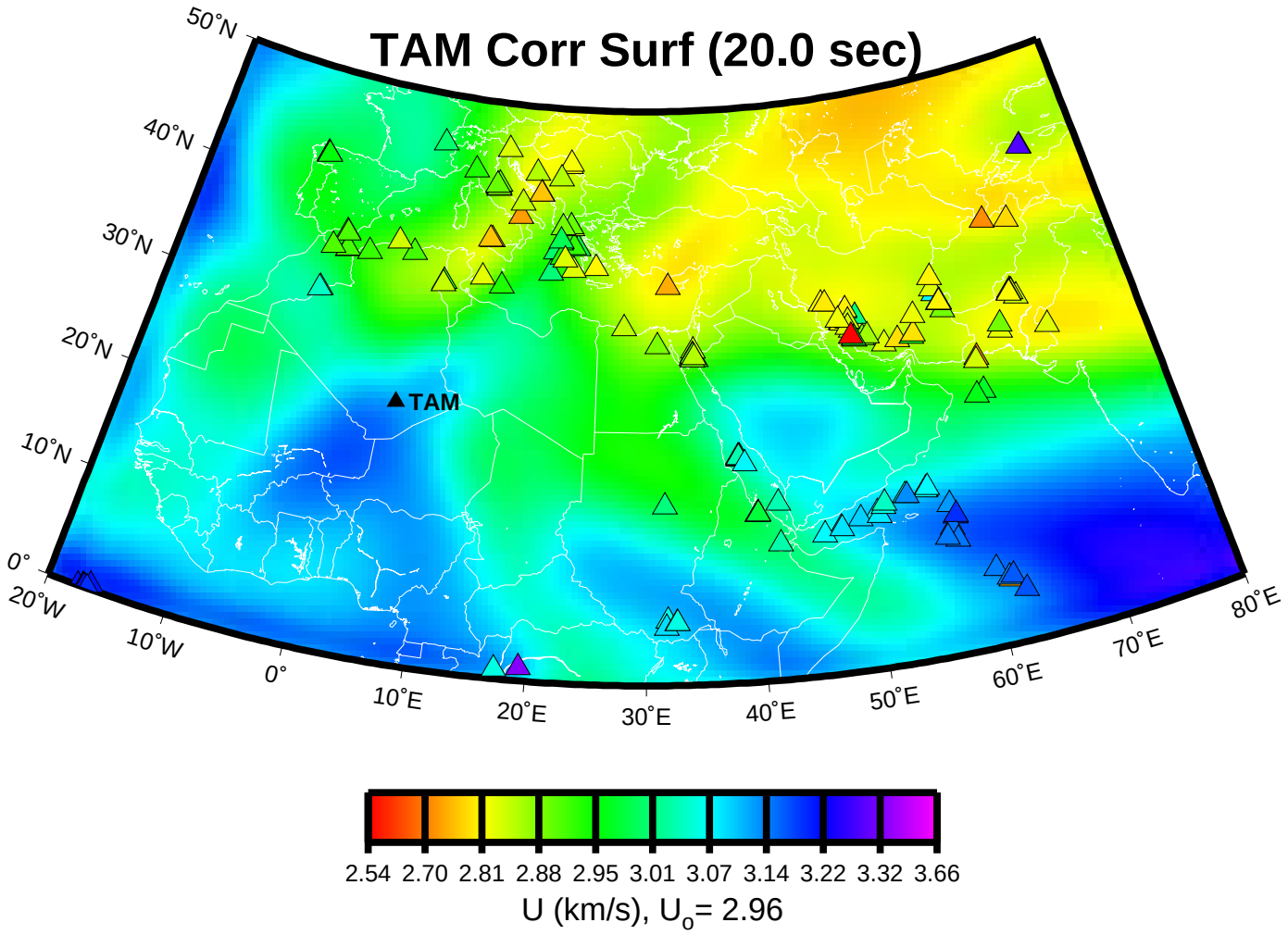
TAM Corr Surf (20.0 sec)
50°N
40°N
30°N
20°N
10°N
0°
20°W
10°W
0°
10°E
20°E
30°E
40°E
50°E
60°E
70°E
80°E
TAM
2.54 2.70 2.81 2.88 2.95 3.01 3.07 3.14 3.22 3.32 3.66
U (km/s), U0= 2.96

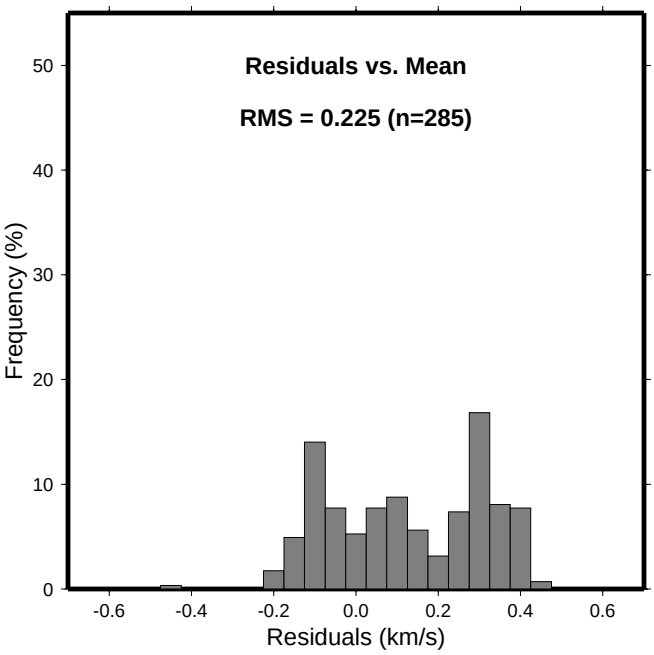
Residuals vs. Mean
RMS = 0.225 (n=285)
Frequency (%)
Residuals (km/s)
0
10
20
30
40
50
-0.6
-0.4
-0.2
0.0
0.2
0.4
0.6

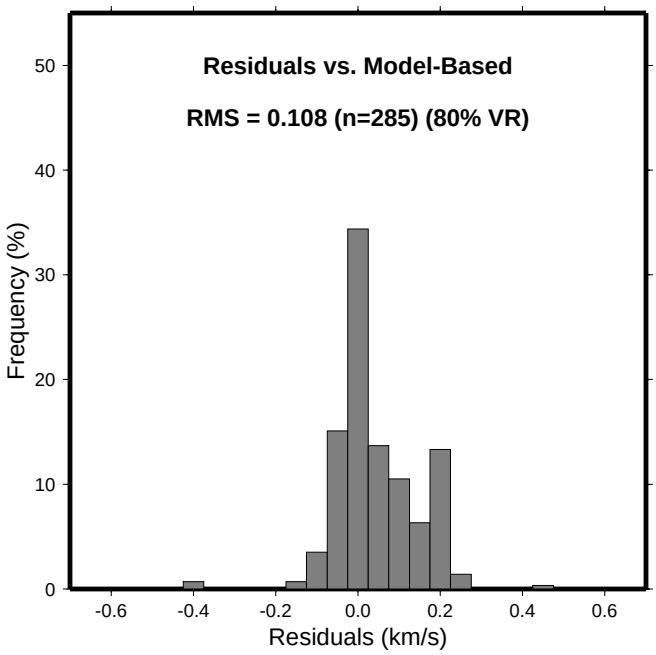
Residuals vs. Model-Based
RMS = 0.108 (n=285) (80% VR)
Frequency (%)
Residuals (km/s)
0
10
20
30
40
50
-0.6
-0.4
-0.2
0.0
0.2
0.4
0.6

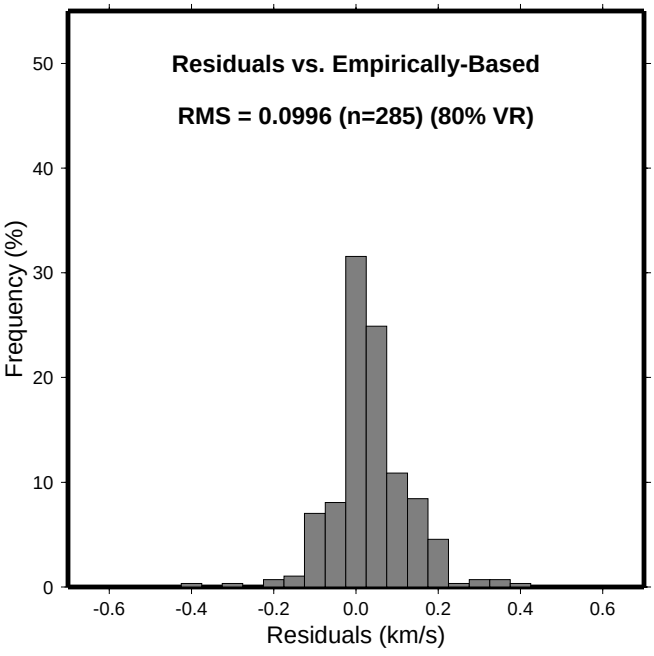
Residuals vs. Empirically-Based
RMS = 0.0996 (n=285) (80% VR)
Frequency (%)
Residuals (km/s)
0
10
20
30
40
50
-0.6
-0.4
-0.2
0.0
0.2
0.4
0.6

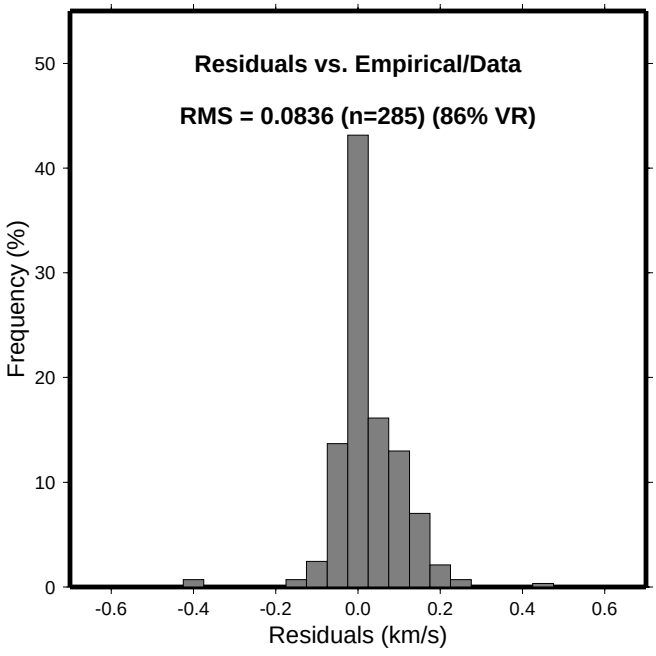
Residuals vs. Empirical/Data
RMS = 0.0836 (n=285) (86% VR)
Frequency (%)
Residuals (km/s)
0
10
20
30
40
50
-0.6
-0.4
-0.2
0.0
0.2
0.4
0.6